

Second-order nonlinear optical effects of spin currents

Jing Wang,^{1,2} Bang-Fen Zhu,^{2,3} and Ren-Bao Liu^{1,*}

¹*Department of Physics, The Chinese University of Hong Kong, Shatin, N.T., Hong Kong, China*

²*Department of Physics, Tsinghua University, Beijing 100084, P.R.China*

³*Institute of Advanced Study, Tsinghua University, Beijing 100084, P.R.China*

Abstract

A pure spin current formed by opposite spins moving in opposite directions is a rank-2 axial tensor which breaks the inversion symmetry. Thus a spin current has a second-order optical susceptibility, with unique polarization-dependence determined by the symmetry properties of the current. In particular, a longitudinal spin current, in which the spin polarization directions are parallel or anti-parallel to the moving directions, being a chiral quantity, leads to a chiral sum-frequency effect. Microscopic calculations based on the eight-band model of a III-V compound semiconductor confirm the symmetry analysis and show that the susceptibility is quite measurable under realistic conditions. The second-order nonlinear optical effects may be used for in-situ and non-destructive detection of spin currents, as a standard spectroscopy tool in research of spintronics.

PACS numbers: 72.25.Dc, 42.65.An, 78.20.Ls

Spin currents, which carry information via spins in lieu of charges, play a key role in spintronics [1, 2]. Pure spin currents also signify the occurrence of some novel spin-related quantum phenomena such as the spin Hall effect [3–10], the quantum spin Hall effect and topological insulators [11–15]. Spin currents were previously observed via spin accumulation at stopping edges [7–9, 16] or conversion to electrical signals [10, 17–19]. Direct and non-destructive measurement of pure spin currents where and while they flow [20, 21] is highly desired, but is very difficult because a pure spin current bears neither net charge current nor net magnetization. Noticing that a longitudinal spin current in which the spins point parallel or anti-parallel to the current is a chiral quantity, we envisaged that it can be probed by the chiral sum-frequency optical spectroscopy which was recently developed to detect molecular chirality [22–24]. By symmetry analysis in general cases and microscopic calculations in realistic models, we discovered that a pure spin current has sizable second-order optical susceptibility. This finding lays the foundation of direct, non-destructive measurement of spin currents by standard optical spectroscopy, facilitating application of spintronics [1, 2] and research on spin-related quantum phenomena [3–15].

As a basic principle of nature, a physical object is measurable only when it breaks certain fundamental symmetries. Indeed, the probe must break the same symmetries as the object does, since the whole coupled system of an object and a probe has the fundamental symmetries. For example, in an Ampère meter, a “pure” charge current, which breaks the time reversal symmetry, is coupled to a microscopic current inside a magnet. Such symmetry consideration led to a scheme of detecting a pure spin current by a “photon spin current” carried by a polarized light beam [20]. A recent experiment [21] showing coupling between a spin current and a spin wave is a remarkable demonstration of the symmetry principle of measurement. Though as a direct probe of spin currents, the spin-wave technique [21] still requires special design and fabrication of magnetic nanostructures and the “photon spin current” probe [20] is limited by weak interaction since it involves the tiny light momentum, these previous works paved the way of searching methods of direct and non-destructive measurement of pure spin currents using symmetry analysis.

Spin currents have peculiar symmetry properties owing to the characteristics of spins. Unlike a charge which is a scalar, a spin is a vector pointing to a certain direction. Physically, a spin is like a tiny magnet resulting from a quantized amount of current circulating about the spin direction [Fig. 1 (a)]. Such physical nature makes a spin an unusual vector, namely, an axial vector. As illustrated in Fig. 1 (a), a spin reverses inside a parallel mirror and is unchanged inside a perpendicular mirror, in opposite to a polar vector. Spin-ups and spin-downs moving in opposite directions

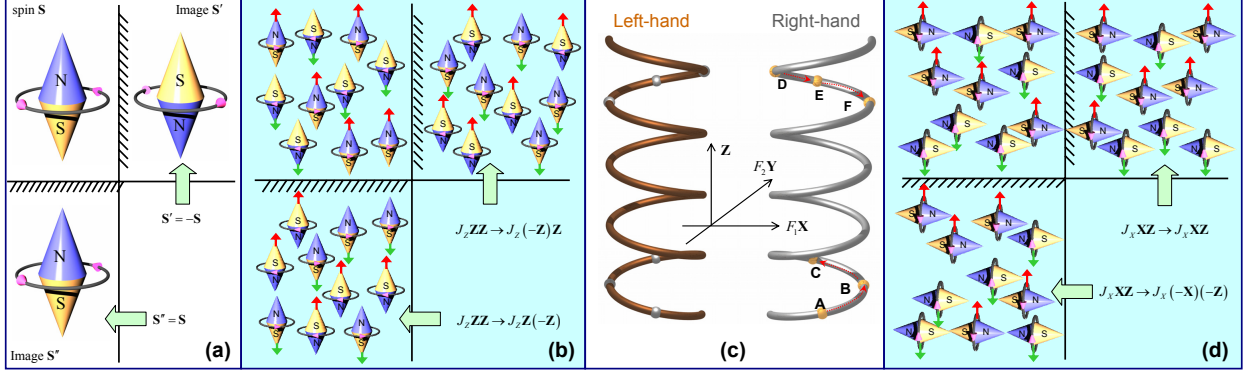


FIG. 1. (Color online) Symmetry analysis for sum-frequency effects of spin currents. (a) A spin under mirror reflections. (b) A longitudinal spin current under mirror reflections. The arrows indicate the moving directions of the spins. (c) Chiral sum-frequency processes in chiral systems. (d) A transverse spin current under mirror reflections.

with the same velocity make up a pure spin current without net spin polarization or magnetization. When the spins are parallel or anti-parallel to the moving direction, the spin current is a longitudinal one. A longitudinal spin current has a special symmetry property - chirality. An object, such as a hand or a helix, is chiral if it cannot be made identical to its mirror image by translation and rotation. The chirality of a longitudinal spin current is illustrated in Fig. 1 (b): If a spin's microscopic current circulates its moving direction left-handedly, the mirror image does right-handedly, and vice versa.

Noticing its chirality, we conceived the idea of measuring a longitudinal spin current using the chiral sum-frequency optical spectroscopy, which was recently developed as a standard tool to study molecular chirality [22–24]. In chiral sum-frequency, two input optical fields \mathbf{F}_1 and \mathbf{F}_2 (with frequencies ω_1 and ω_2 , respectively) and the induced polarization field \mathbf{P} at frequency $\omega_1 + \omega_2$ form a left- or right-hand system. Fig. 1 (c) shows how a chiral sum-frequency process occurs in a chiral system. Considering a right-hand helix, a charge at position A will be driven to point B by an electric field \mathbf{F}_1 which is along the X-axis, and then to point C by \mathbf{F}_2 which is along the Y-axis. The confinement of the helix leads to a net displacement along the Z-axis. Thus the two input fields and the induced polarization ($\mathbf{F}_1, \mathbf{F}_2, \mathbf{P}$) form a right-hand system. If the order of input fields is reversed (\mathbf{F}_2 applies before \mathbf{F}_1), the charge would follow a trajectory like $D \rightarrow E \rightarrow F$, resulting in a polarization along the $-Z$ -axis, and ($\mathbf{F}_2, \mathbf{F}_1, \mathbf{P}$) still form a right-hand system. Similarly, the sum-frequency in a left-hand helix is a left-hand chiral process. A sum-

frequency process is characterized by a second-order susceptibility $\chi^{(2)}$ via $\mathbf{P}(\omega_1 + \omega_2) = \chi^{(2)} : \mathbf{F}_1(\omega_1) \mathbf{F}_2(\omega_2)$. In the above example of helix, the susceptibility may be written as a form of three dyadic vectors, $\chi^{(2)} = A(\mathbf{Z}\mathbf{Y}\mathbf{X} - \mathbf{Z}\mathbf{X}\mathbf{Y})$, i.e., a rank-3 tensor. Thus the chiral sum-frequency susceptibility provides a measurement of the chirality of a physical object. If otherwise measured in linear optics, the effect of the molecular chirality relies on the small magnetic moment of the molecules, and in turn on the small photon momentum of the probe light, similar to the case of linear optical effects of spin currents [20].

For a systematic symmetry analysis, we consider a spin current with both longitudinal and transverse components. We define the Z -axis as the current direction and the X -axis as the spin direction of the transverse component. The spin current can be written as a rank-2 tensor $\mathbb{J} = J_X \mathbf{X}\mathbf{Z} + J_Z \mathbf{Z}\mathbf{Z}$, in a form of dyadic vectors, in which the left/right vector is the spin/current direction and $J_{Z/X}$ is the longitudinal/transverse amplitude. Above all, the spin current breaks the inversion symmetry, satisfying the symmetry properties required by a second-order optical process [25].

In general, the sum-frequency susceptibility tensor has 27 independent terms, $\chi^{(2)} = \chi_{XXX} \mathbf{X}\mathbf{X}\mathbf{X} + \chi_{XXY} \mathbf{X}\mathbf{X}\mathbf{Y} + \dots + \chi_{ZZZ} \mathbf{Z}\mathbf{Z}\mathbf{Z}$, but the symmetry properties of a spin current will set many terms to be zero or non-independent [25]. For a longitudinal spin current, only the chiral terms are non-zero. In a non-chiral term, at least one of the three directions \mathbf{X} , \mathbf{Y} and \mathbf{Z} appears even times (twice or zero times). Consider $\chi_{XXY} \mathbf{X}\mathbf{X}\mathbf{Y}$ for example. Under reflection by the Y - Z plane, the longitudinal spin current is reversed, but $\chi_{XXY} \mathbf{X}\mathbf{X}\mathbf{Y}$ is unchanged, so this term must be zero. Similar arguments apply to other non-chiral terms. Also, the susceptibility must be anti-symmetric under reflection by any plane parallel to the Z -axis. With these constraints, the sum-frequency susceptibility of a longitudinal spin current can be written as

$$\chi_{J_Z}^{(2)} = J_Z \left[\alpha_1 (\mathbf{X}\mathbf{Y}\mathbf{Z} - \mathbf{Y}\mathbf{X}\mathbf{Z}) + \alpha_2 (\mathbf{Y}\mathbf{Z}\mathbf{X} - \mathbf{X}\mathbf{Z}\mathbf{Y}) + \alpha_3 (\mathbf{Z}\mathbf{X}\mathbf{Y} - \mathbf{Z}\mathbf{Y}\mathbf{X}) \right], \quad (1)$$

with only three independent parameters. As for a transverse spin current $J_X \mathbf{X}\mathbf{Z}$, it changes its sign under reflection by the X - Z plane but is invariant under reflection by the X - Y or Y - Z plane [see Fig. 1 (d)], each non-zero term in the susceptibility must contain odd times of \mathbf{Y} and even times of \mathbf{Z} or \mathbf{X} , so

$$\chi_{J_X}^{(2)} = J_X (x_1 \mathbf{X}\mathbf{X}\mathbf{Y} + x_2 \mathbf{X}\mathbf{Y}\mathbf{X} + x_3 \mathbf{Y}\mathbf{X}\mathbf{X} + z_1 \mathbf{Z}\mathbf{Z}\mathbf{Y} + z_2 \mathbf{Z}\mathbf{Y}\mathbf{Z} + z_3 \mathbf{Y}\mathbf{Z}\mathbf{Z} + y \mathbf{Y}\mathbf{Y}\mathbf{Y}), \quad (2)$$

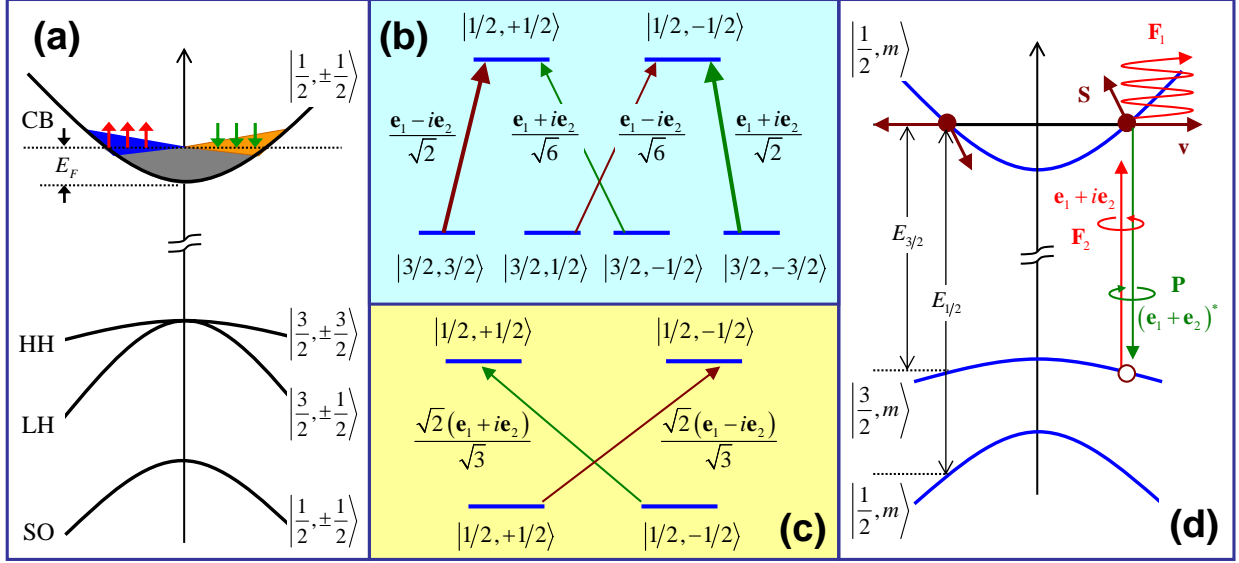


FIG. 2. (Color online) Models for microscopic calculation of the sum-frequency susceptibility. (a) The full eight-band model and the electron spin distribution for a pure spin current in a semiconductor. (b) and (c) Selection rules and relative dipole moments from the spin-3/2 and spin-1/2 valence bands to the conduction band, respectively. (d) A simplified model with the HH-LH splitting neglected. The spin states and selection rules for inter-band transitions are independent of the momentum. The transition energies to the Fermi surface from different valence bands are indicated.

with seven independent parameters. The unique polarization-dependence of the second-order susceptibility of a spin current can be used to distinguish its transverse and longitudinal components, and also to single out the spin-current signature from the effects of the material background or a charge current [26].

To determine the independent parameters of the susceptibility in Eqns. (1) and (2), we performed microscopic calculation for a pure spin current in a bulk GaAs, using the standard perturbation theory [25, 27] with an eight-band model [28]. We assumed that the pure spin current result from a non-equilibrium distribution of electrons in the conduction band, with a small portion of electrons near the Fermi surface having opposite spin polarizations for opposite velocities [Fig. 2 (a)], under conditions similar to those in Ref. [7]. The optical interaction includes the inter-band transitions between the valence bands and the conduction band and the intra-band acceleration of electrons and holes. To avoid real absorption of light, the light frequencies were chosen such that the sum frequency is below the band gap. For the sake of simplicity, we neglected the anisotropy of the valence bands. We also adopted the free-particle approximation,

which is justified since the Coulomb interaction is largely screened in the n-doped material. These approximations, according to the symmetry analysis, would only quantitatively modify the results. The spin splitting due to the bulk inversion asymmetry of the material (the Dresselhaus effect) is as small as 0.01 meV for the doping level considered ($3 \times 10^{16} \text{ cm}^{-3}$), and therefore was neglected in the calculation. The bulk inversion asymmetry would cause a background second-order susceptibility, which is indeed strong but can be well separated from the spin-current effect by AC modulation of the current and phase-locking detection. Two representative results of the calculated susceptibility spectra are shown in Figs. 3 (a) and (b). The other terms of the susceptibility tensor (not shown) have similar frequency-dependence and comparable amplitudes. As a specific example, a transverse spin current $20 \text{ nA}/\mu\text{m}^{-2}$ has a susceptibility $\chi_{YZZ} \approx 0.40 \times 10^{-9} \text{ esu}$ (or $0.17 \times 10^{-12} \text{ m/V}$ in SI units) for input frequencies $\omega_1 = 100 \text{ meV}$ and $\omega_2 = 1,400 \text{ meV}$, or $17. \times 10^{-12} \text{ esu}$ for $\omega_1 = \omega_2 = 750 \text{ meV}$ (corresponding to the second harmonics generation).

To better understand the microscopic mechanism of the sum-frequency effect of a spin current, we simplify the model by neglecting the splitting between the heavy hole (HH) band and the light hole (LH) band. Under this approximation, the HH and LH bands form a spin-3/2 band with 4-fold degeneracy. The split-off (SO) band and the conduction band have spin-1/2. In this simplified model, the spin states and the selection rules for inter-band transitions are separated from the momentum [Figs. 2 (b) and (c)].

Let us first consider a single electron with momentum \mathbf{k} and spin polarization $\mathbf{s}_\mathbf{k}$ [Fig. 2 (d)]. We set up a coordinate system ($\mathbf{e}_1, \mathbf{e}_2, \mathbf{e}_3$) so that $\mathbf{s}_\mathbf{k} = \mathbf{e}_3 (f_+ - f_-) / 2$ with $f_{+/-}$ denoting the population at the spin-up/down state. The angular momentum conservation requires that a light with circular polarization $\mathbf{e}_1 \pm i\mathbf{e}_2$ couples only to the transitions $|j, m\rangle \leftrightarrow |1/2, m \pm 1\rangle$, where $j = 3/2$ or $1/2$ is the spin of a valence band and $m = -j, j + 1, \dots$, or j is the component along the \mathbf{e}_3 -axis. The relative dipole moments of the relevant inter-band transitions are indicated in Figs. 2 (b) and (c). To simplify the discussion, we set the input frequency ω_2 to be near resonant with the band gap and much greater than ω_1 , so that the inter-band transitions and the intra-band driving are mostly caused by $\mathbf{F}_2 \exp(-i\omega_2 t_2)$ and $\mathbf{F}_1 \exp(-i\omega_1 t_1)$, respectively.

The probability amplitude of a certain inter-band transition is determined by the inner product of the dipole moment and the optical field. For example, the transition $|3/2, -3/2\rangle \rightarrow |1/2, 1/2\rangle$ generated between t_2 and $t_2 + dt_2$ has a probability amplitude $dG_2 = i(1 - f_-) (d_{cv}^* / \sqrt{2}) (\mathbf{e}_1 + i\mathbf{e}_2) \cdot \mathbf{F}_2 \exp(-i\omega_2 t_2) dt_2$, where d_{cv} is the inter-band dipole, and the factor $(1 - f_-)$ accounts for the Pauli blocking. After the excitation, the probability amplitude oscillates in time with frequency

$E_{3/2}(\mathbf{k})$, leading to the optical polarization $(\mathbf{e}_1 + i\mathbf{e}_2)(d_{cv}/\sqrt{2})e^{-iE_{3/2}(\mathbf{k})(t-t_2)}dG_2$ at time t , where $E_{3/2}(\mathbf{k}) = k^2/(2m_e) + k^2/(2m_{3/2})$ is the transition energy of a pair of electron and hole with mass m_e and $m_{3/2}$, respectively. The radiation has the same circular polarization as the input because of the angular momentum conservation. Summation over all possible transitions and integration over time give the linear optical response to the field \mathbf{F}_2 as

$$\begin{aligned} \mathbf{P}^{(1)}(t) = & \frac{i}{3} |d_{cv}|^2 \int_{-\infty}^t e^{-iE_{3/2}(\mathbf{k})(t-t_2)} \\ & \times \sum_{\pm} (1 - f_{\pm}) (\mathbf{e}_1 \mp i\mathbf{e}_2) (\mathbf{e}_1 \mp i\mathbf{e}_2)^* \cdot \mathbf{F}_2 e^{-i\omega_2 t_2} dt_2. \end{aligned} \quad (3)$$

Thus $\mathbf{P}^{(1)} \propto \mathbf{s}_{\mathbf{k}} (\mathbf{e}_1 \mathbf{e}_2 - \mathbf{e}_2 \mathbf{e}_1) \cdot \mathbf{F}_2 = \mathbf{F}_2 \times \mathbf{s}_{\mathbf{k}}$, which has a transparent physical meaning: The linear polarization of the output field is related to that of the input one by a rotation about the spin, essentially a Faraday rotation due to the spin acting as a magnet. When the effect of the intra-band driving by \mathbf{F}_1 is included, the momentum k should be replaced with the accelerated one $\tilde{\mathbf{k}}_{\tau} \equiv \mathbf{k} - e\mathbf{F}_1 \int_{-\infty}^{\tau} \exp(-i\omega_1 t_1) dt_1$ at time τ , and the phase $E_{3/2}(\mathbf{k})(t - t_2)$ accumulated from the creation time t_2 to the recombination time t should be replaced with $\int_{t_2}^t E_{3/2}(\tilde{\mathbf{k}}_{\tau}) d\tau$. By expansion to the linear order of \mathbf{F}_1 , we have $\tilde{k}_{\tau}^2 \approx k^2 - 2e\mathbf{k} \cdot \mathbf{F}_1 \int_{-\infty}^{\tau} \exp(-i\omega_1 t_1) dt_1$, so the second-order optical response can be written as $\mathbf{P} \propto \mathbf{F}_2 \times \mathbf{s}_{\mathbf{k}} e\mathbf{v}_{\mathbf{k}} \cdot \mathbf{F}_1$, where $\mathbf{v}_{\mathbf{k}} \equiv \mathbf{k}/m_e$ is the velocity of the electron with momentum \mathbf{k} . The physical meaning of $e\mathbf{v}_{\mathbf{k}} \cdot \mathbf{F}_1$ is obviously the power done by the field to the electron. $e\mathbf{s}_{\mathbf{k}}\mathbf{v}_{\mathbf{k}}$ is just the spin current tensor contributed by the electron.

For a distribution of electrons, the summation over the momentum space gives the sum-frequency response as $\mathbf{P} = \zeta \mathbf{F}_2 \times (\mathbb{J} \cdot \mathbf{F}_1)$, with

$$\begin{aligned} \zeta = & \left(\frac{\epsilon_r + 2}{3} \right)^3 \frac{(2/3) |d_{cv}|^2 (1 + m_e/m_{3/2})}{(\omega_1 + \omega_2 - E_{3/2})(\omega_2 - E_{3/2}) \omega_1} \\ & - \left(E_{3/2}, m_{3/2} \rightarrow E_{1/2}, m_{1/2} \right), \end{aligned} \quad (4)$$

derived by Fourier transformation of Eq. (3) including the intra-band driving and the contribution of the SO band, where the factor containing the material dielectric constant ϵ_r takes into account the difference between the macroscopic external field and the microscopic local field [29], m_j denotes the mass of the spin- j hole band, and E_j is the transition energy from the spin- j band to the Fermi surface [see Fig. 2 (d)]. The constants in Eqns. (1) and (2) are such that $\alpha_1 = -z_2 = z_3 = \zeta$ and others = 0. With the HH-LH splitting neglected, the sum-frequency susceptibility has a compact form with only one independent parameter. This feature is due to the separation of the spin and motion degrees of freedom of the electrons and holes. When the HH-LH splitting

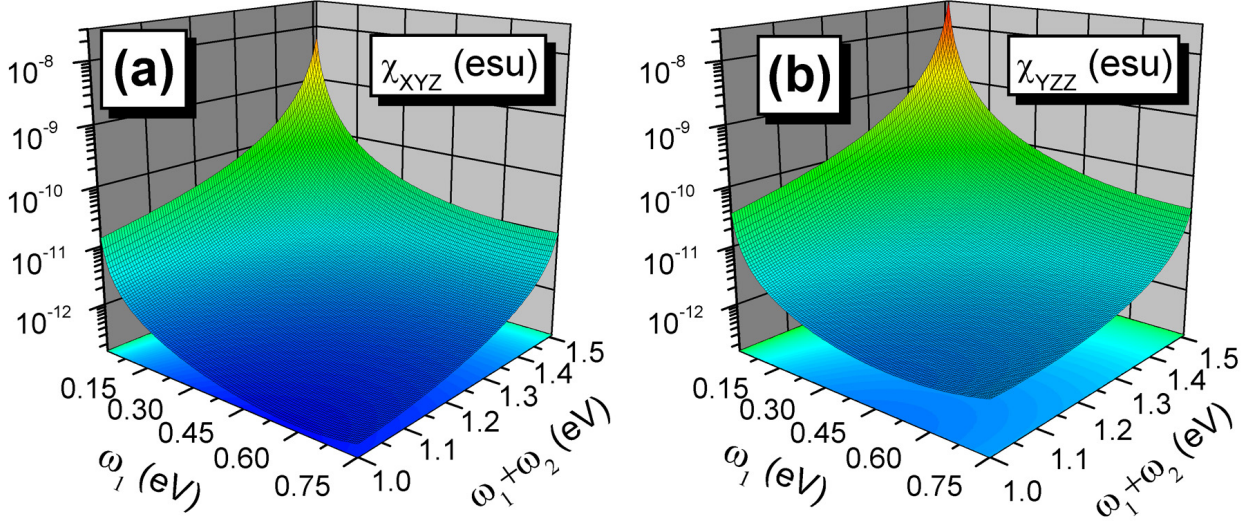


FIG. 3. (Color online) Representative results of the sum-frequency susceptibility. (a) χ_{XYZ} due to a longitudinal spin current, and (b) χ_{YZZ} due to a transverse spin current, as functions of the optical frequencies. Parameters are chosen similar to those in Ref. [7]: The band gap is 1519 meV, the HH-SO splitting is 341 meV, the doping concentration is $3 \times 10^{16} \text{ cm}^{-3}$, the effective mass (in units of free electron mass) of the HH, LH, SO, and conduction bands is in turn 0.45, 0.082, 0.15, and 0.067, the dipole $d_{cv} = 6.7 \text{ e}\text{\AA}$, the dielectric constant $\epsilon_r = 10.6$, and the spin current $J_X = J_Z = 20 \text{ nA}/\mu\text{m}^2$.

is non-zero, the spin quantization direction and therefore the optical selection rules depend on the momentum and vary with acceleration of the particles. This leads to the general form of susceptibility in Eqns. (1) and (2), with the extra terms proportional to the HH-LH splitting.

In summary, with systematic symmetry analysis in general cases and microscopic calculation under realistic conditions, we have shown that a pure spin current has a sizable sum-frequency susceptibility. In particular, a longitudinal spin current has a chiral sum-frequency effect. The current results can be straightforwardly extended to other second-order optical spectroscopy such as difference-frequency and three-wave mixing [25]. Thus the standard nonlinear optical spectroscopy makes up a toolbox for research of spintronics. With universality of the method guaranteed by the symmetry principle and without requirements of resonance conditions or special structure design and fabrication, the nonlinear optical spectroscopy can be applied to study a wide range of spin-related quantum phenomena such as the quantum spin Hall effect and topological insulators [11–15]. A wealth of physics connecting spins and photons and technologies synthesizing spintronics and photonics are still to be explored.

This work was supported by Hong Kong RGC HKU 10/CRF/08, Hong Kong GRF CUHK 402207, the NSFC Grant Nos. 10774086, 10574076 and the Basic Research Program of China Grant No. 2006CB921500.

* To whom correspondence should be addressed. Email: rblu@phy.cuhk.edu.hk

- [1] S. A. Wolf, D. D. Awschalom, R. A. Buhrman, J. M. Daughton, S. von Molnár, M. L. Roukes, A. Y. Chtchelkanova, and D. M. Treger, *Science* **294**, 1488 (2001).
- [2] I. Zutic, J. Fabian, and S. Das Sarma, *Rev. Mod. Phys.* **76**, 323 (2004).
- [3] M. I. Dyakonov, V. I. Perel, *Phys. Lett. A* **35**, 459 (1971).
- [4] J. E. Hirsch, *Phys. Rev. Lett.* **83**, 1834 (1999).
- [5] S. Murakami, N. Nagaosa, and S. C. Zhang, *Science* **301**, 1348 (2003).
- [6] J. Sinova, D. Culcer, Q. Niu, N. A. Sinitsyn, T. Jungwirth, and A. H. MacDonald, *Phys. Rev. Lett.* **92**, 126603 (2004).
- [7] Y. K. Kato, R. C. Myers, A. C. Gossard, and D. D. Awschalom, *Science* **306**, 1910 (2004).
- [8] J. Wunderlich, B. Kaestner, J. Sinova, and T. Jungwirth, *Phys. Rev. Lett.* **94**, 047204 (2005).
- [9] H. Zhao, E. J. Loren, H. M. van Driel, and A. L. Smirl, *Phys. Rev. Lett.* **96**, 246601 (2006).
- [10] S. O. Valenzuela and M. Tinkham, *Nature* **442**, 176 (2006).
- [11] C. L. Kane and E. J. Mele, *Phys. Rev. Lett.* **95**, 226801 (2005).
- [12] B. A. Bernevig, T. L. Hughes, and S. C. Zhang, *Science* **314**, 1757 (2006).
- [13] M. König, S. Wiedmann, C. Brüne, A. Roth, H. Buhmann, L. W. Molenkamp, X. L. Qi, and S. C. Zhang, *Science* **318**, 766 (2007).
- [14] D. Hsieh, Y. Xia, D. Qian, L. Wray, J. H. Dil, F. Meier, J. Osterwalder, L. Patthey, J. G. Checkelsky, N. P. Ong, A. V. Fedorov, H. Lin, A. Bansil, D. Grauer, Y. S. Hor, R. J. Cava, and M. Z. Hasan, *Nature* **460**, 1101 (2009).
- [15] P. Roushan, J. Seo, C. V. Parker, Y. S. Hor, D. Hsieh, D. Qian, A. Richardella, M. Z. Hasan, R. J. Cava, and A. Yazdani, *Nature* **460**, 1106 (2009).
- [16] M. J. Stevens, A. L. Smirl, R. D. R. Bhat, A. Najmaie, J. E. Sipe, and H. M. van Driel, *Phys. Rev. Lett.* **90**, 136603 (2003).
- [17] I. Appelbaum, B. Q. Huang, and D. J. Monsma, *Nature* **447**, 295 (2007).
- [18] S. D. Ganichev, S. N. Danilov, V. V. Bel'kov, S. Giglberger, S. A. Tarasenko, E. L. Ivchenko, D. Weiss,

- W. Jantsch, F. Schäffler, D. Gruber, and W. Prettl, Phys. Rev. B **75**, 155317 (2007).
- [19] X. D. Cui, S.-Q. Shen, J. Li, Y. Ji, W. Ge, and F.-C. Zhang, Appl. Phys. Lett. **90**, 242115 (2007).
- [20] J. Wang, B. F. Zhu, and R. B. Liu, Phys. Rev. Lett. **100**, 086603 (2008); see also Erratum, *ibid* **101**, 069902 (2008).
- [21] V. Vlamincck and M. Bailleul, Science **322**, 410 (2008).
- [22] M. A. Belkin, T. A. Kulakov, K. H. Ernst, L. Yan, and Y. R. Shen, Phys. Rev. Lett. **85**, 4474 (2000).
- [23] J. Wang, X. Y. Chen, M. L. Clarke, and Z. Chen, Proc. Nat. Acad. Sci. USA **102**, 4978 (2005).
- [24] N. Ji, V. Ostroverkhov, M. Belkin, Y. J. Shiu, and Y. R. Shen, J. Am. Chem. Soc. **128**, 8845 (2006).
- [25] Y. R. Shen, *The Principles of Nonlinear Optics* (Wiley-Interscience, New York, 1984).
- [26] J. B. Khurgin, Appl. Phys. Lett. **67**, 1113 (1995).
- [27] J. E. Sipe and A. I. Shkrebtii, Phys. Rev. B **61**, 5337 (2000).
- [28] P. Y. Yu and M. Cardona, *Fundamentals of Semiconductors: Physics and Material Properties*, 3rd ed. (Springer-Verlag, Berlin, 2005).
- [29] N. Bloembergen, *Nonlinear Optics* (Benjamin, New York, 1965).